nature photonics

ARTICLES

PUBLISHED ONLINE: 13 JULY 2014 | DOI: 10.1038/NPHOTON.2014.151

Reduced spin measurement back-action for a phase sensitivity ten times beyond the standard quantum limit

J. G. Bohnet†, K. C. Cox, M. A. Norcia, J. M. Weiner, Z. Chen† and J. K. Thompson*

Fundamental quantum noise limits the precision of quantum-based detectors, for example limiting the ultimate precision of atomic clocks, which have applications in communication, navigation and tests of fundamental physics. Collective measurements of many quantum spins can project the ensemble into an entangled, spin-squeezed state with improved quantum-limited measurement resolution. However, measurement back-action has limited previous implementations of collective measurements to only modest observed enhancements in precision. Here, we experimentally demonstrate a collective measurement with reduced measurement back-action to produce and directly observe, with no background subtraction, a spin-squeezed state with phase resolution improved by a factor of 10.5(1.5) in variance, or 10.2(6) dB, compared to the initially unentangled ensemble of $N = 4.8 \times 10^5$ ^{87}Rb atoms. The measurement uses a cavity-enhanced probe of an optical cycling transition, mitigating back-action associated with state-changing transitions induced by the probe. This work establishes collective measurements as a powerful technique for generating useful entanglement for precision measurements.

A defining characteristic of quantum mechanics is the ability of a measurement to change the state of the system being measured. For example, a measurement of a system in a superposition of two states causes the system to project, or collapse, into one of the two discrete states. Measurements performed on an ensemble, however, can project the ensemble into an entangled state when only collective quantities are measured. In contrast, any information about the spin state of a single atom that leaks to the environment due to imperfections in the collective measurement reduces entanglement due to the collapse of the quantum spin state of individual atoms. Collective or joint measurements arise in a wide range of applications, including quantum teleportation[1], quantum information protocols[2], studies of strongly correlated quantum systems[3], Dicke superradiance[4] and entanglement generation in optical[5], solid-state[6] and atomic systems[7].

Entanglement generated by a collective measurement can be used to overcome the fundamental quantum randomness that limits a diverse set of precision measurements[8]. Atomic sensors in particular are nearly or already limited by atomic quantum noise, so entanglement-enhanced metrology may improve some of the most precise measurements of external fields[9], rotations[10] and time[11,12], and will advance searches for new physics[13].

Atomic sensors encode information in a quantum phase θ, the value of which is estimated by measuring the population of atoms in different quantum states. Quantum projection noise[14] for an ensemble of N independent atoms limits the uncertainty in the estimate of θ to a variance $\Delta\theta^2 \geq \Delta\theta^2_{\mathrm{SQL}} = 1/N$, a limit known as the standard quantum limit (SQL) for a coherent spin state (CSS). Entanglement can be used to bypass this limitation in atomic sensors, as well as in microwave[15] and optical[16] fields.

A collective measurement that both resolves the quantum noise that appears in θ and also induces sufficiently small measurement back-action can be used to subtract quantum noise from subsequent measurements of θ (ref. 8). Although the resulting state of the ensemble is termed a conditional spin-squeezed state, the reduction in noise is completely deterministic with no discarding of trials necessary. The improvement in phase estimation relative to the SQL is quantified by the observed spectroscopic enhancement[17], $W^{-1} \equiv (\Delta\theta_{\mathrm{SQL}}/\Delta\theta)^2$. $W^{-1} > 1$ also guarantees that the state is entangled.

First proof-of-principle experiments using collective pre-measurements have shown that entanglement can enhance the sensitivity of an atomic ensemble[18–22]. However, measurement-induced back-action, including loss of sensitivity due to decoherence and noise due to population diffusion between states, has limited the direct observations of spectroscopic enhancement to only $W^{-1} \leq 1.4$ (ref. 20). Such a small spectroscopic enhancement is probably not worthwhile for application in precision measurements.

In this Article, we utilize cavity-based, collective pre-measurements with reduced back-action by probing the atoms on a cycling transition to achieve a directly observed spectroscopic enhancement $W^{-1} = 10.5(1.5)$ in an ensemble of $N = 4.8 \times 10^5$ ^{87}Rb atoms (Fig. 1a). The techniques demonstrated here are well suited to state-of-the-art optical lattice clocks[11,12], which have even more favourable cycling transitions than the one exploited here. We emphasize that our result reflects no background subtraction or corrections for finite probe detection efficiency. Reporting the actual observed spectroscopic enhancement is critical for establishing that entangled states are more than a physical novelty and may actually be applied to enhance real measurements. In previous work, performing background subtractions would often tease out physically interesting quantum effects, while the actual spectroscopic enhancement was relatively small.

Entanglement-enhanced states have also been generated for small ($N \leq 14$) collections of atomic ions using quantum-logic operations[23–26] and for larger neutral atomic ensembles using atomic

JILA, University of Colorado and NIST, Boulder, Colorado 80309, USA; †Present addresses: National Institute of Standards and Technology, Boulder, Colorado 80305, USA (J.G.B.), Data Storage Institute, Agency for Science, Technology and Research, Singapore 117608, Singapore (Z.C.).
*e-mail: jkt@jila.colorado.edu

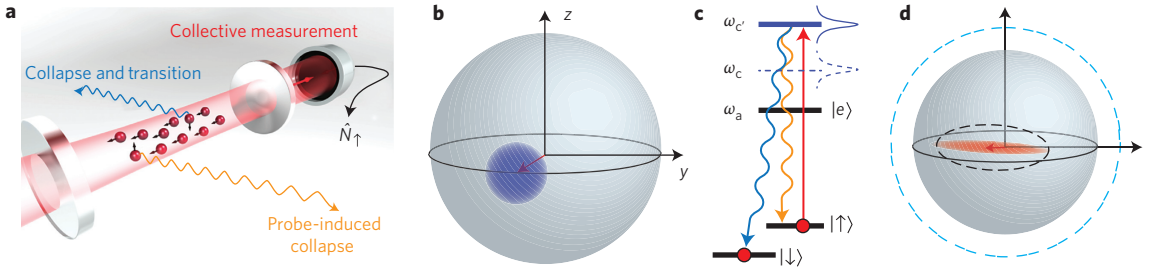

Figure 1 | Spin-squeezing and measurement back-action. a, Atoms collectively interact with light in an optical cavity. A measurement of the phase of the probe field (red) is sensitive to the total number of atoms in spin up, and projects the ensemble into an entangled state, conditioned on the measurement outcome. Probe photons can be scattered into free space, causing atoms to collapse to spin up (orange wavy lines in **a** and **c**) and can also cause state-changing transitions (blue wavy lines in **a** and **c**). **b**, A coherent spin state can be visualized by a Bloch vector (red), with a pointing uncertainty set by quantum noise, represented by the blue shaded region at the tip of the vector. The transparent sphere represents the surface on which the tip of the Bloch vector resides if rotated. **c**, An energy-level diagram of the collective measurement. Atoms in $|\uparrow\rangle$ with optical transition frequency ω_a off-resonantly couple to the detuned cavity mode with resonance frequency ω_c. The coupling results in a dressed cavity mode with resonant frequency $\omega_{c'}$, so probing $\omega_{c'}$ measures the total number of atoms in $|\uparrow\rangle$, and hence the Bloch vector's spin projection J_z, without measuring the state of individual atoms. Probing on a cycling transition suppresses back-action from scattering events that change an atom's state to $|\downarrow\rangle$ (blue), limiting back-action to collapse (orange). **d**, After a pre-measurement, back-action modifies the noise distribution of the Bloch vector. The uncertainty of the J_z projection decreases, but fundamental measurement back-action increases the uncertainty along $\hat{y}$ as required by Heisenberg uncertainty relations. The non-ideal back-action caused by free-space scattering is indicated by dashed lines. State collapse reduces the length J of the collective Bloch vector, with the effect illustrated by the dashed blue line. In addition, those free-space scattering events that cause a state-changing transition result in added noise in J_z, indicated by the dashed black ellipse around the Bloch vector.

collisions[27–32] or cavity-mediated optical feedback[33]. Directly observed enhancements of up to $W^{-1} = 5.0(1)$, 7(1) and 3.6(5) (at $N = 8$, 4.5×10^4 and 3×10^4) have been realized using these respective approaches[25,32,33]. Although the largest observed spectroscopic enhancement reported prior to our work was obtained in squeezed states generated with collisional interactions, applying this entanglement to perform enhanced measurements remains to be explored. Unless the collisional interactions can be precisely extinguished, the collisional interactions that generate the squeezing can also result in systematic errors of the measured quantity and the loss of the useful entanglement during the sensing phase. Using an optical approach, potential perturbations are only present during the pre-measurement.

Experimental system and collective measurement

Our experimental system[34] consists of an ensemble of N pseudo-spin-1/2s formed by the hyperfine ground states $|\uparrow\rangle \equiv |F = 2, m_f = +2\rangle$ and $|\downarrow\rangle \equiv |F = 1, m_f = +1\rangle$ in ^{87}Rb, separated by 6.8 GHz. The quantum state of the ensemble can be approximated as a single collective spin or Bloch vector $\mathbf{J} \equiv \langle\hat{\mathbf{J}}\rangle$, in an abstract space defined by the collective spin operator $\hat{\mathbf{J}} = \hat{J}_x\hat{x} + \hat{J}_y\hat{y} + \hat{J}_z\hat{z}$ (Fig. 1b; see Supplementary Section I). The spin projection operator $\hat{J}_z = \hat{N}_\uparrow - N/2$ can be written in terms of the measurable quantities: the total atom number N and the spin-up population operator $\hat{N}_\uparrow = \Sigma_{i=1}^{N} |\uparrow_i\rangle\langle\uparrow|$, where i labels individual atoms. The length of the vector is $J = |\langle\hat{\mathbf{J}}\rangle|$. For an unentangled CSS, $J = N/2$.

The quantum projection noise and standard quantum limit can be understood as arising from uncertainty in the orientation of the Bloch vector (Fig. 1b). This quantum uncertainty can be visualized as a quasi-probability distribution perpendicular to the mean vector. When the Bloch vector is oriented along $\hat{x}$, the degree of uncertainty in the orthogonal spin projections is constrained by a Heisenberg uncertainty relationship $\Delta J_z \Delta J_y \geq N/4$, where ΔX indicates the standard deviation of repeated measurements of X. For a CSS of atoms $\Delta J_z = \Delta J_y = \Delta N_{CSS} = \sqrt{N}/2$, and so the SQL for the angle $\theta \approx J_z/J = 2N_\uparrow/N - 1$ is set by the projection noise fluctuations to $\Delta\theta_{SQL} = 1/\sqrt{N}$.

The conditionally squeezed state is created by first preparing a CSS along $\hat{x}$ and then making a collective pre-measurement of $\hat{N}_\uparrow$, with measurement outcome labelled $N_{\uparrow p}$ and subtracting the result from a subsequent final measurement of $\hat{N}_\uparrow$, labelled $N_{\uparrow f}$. The differential quantity $N_{\uparrow f} - N_{\uparrow p}$ can possess reduced noise relative to the projection noise fluctuations ΔN_{CSS} appearing in the two separate measurements. The spin noise reduction is calculated as $R = (\Delta(N_{\uparrow f} - N_{\uparrow p}))^2/\Delta N_{CSS}^2$. By making a collective or joint measurement, any rotation of the vector's polar angle θ that occurs between the two measurements will still modify the differential quantity $N_{\uparrow f} - N_{\uparrow p}$, leading to the desired enhancement in the estimation of applied phase shifts.

To measure the collective state population $N_\uparrow$, the atomic ensemble is coupled to the $TEM_{0,0}$ mode of an optical cavity. The coupling is characterized by an effective single-atom Rabi frequency $2g = 2\pi \times 894(46)$ kHz. The details of inhomogeneous coupling to the probe in our standing-wave cavity are handled as in refs 19 and 21. With no atoms present, the cavity has a resonant frequency ω_c and decay rate $\kappa = 2\pi \times 11.8(1)$ MHz. We detune the cavity frequency from an atomic transition by $\delta = \omega_c - \omega_a = 2\pi \times 200$ MHz, where ω_a is the frequency of the atomic transition from $|\uparrow\rangle$ to an optically excited state $|e\rangle \equiv |F = 3', m_f = +3\rangle$. The radiative decay rate of $|e\rangle$ in free space is $\Gamma = 2\pi \times 6.07$ MHz. Atoms in $|\uparrow\rangle$ produce a dressed atom-cavity resonance at frequency $\omega_{c'}$, such that $\omega_{c'} - \omega_c = \left(\sqrt{\delta^2 + 4g^2 N_\uparrow} - \delta\right)/2$ (Fig. 1c; see Supplementary Section II). We measure $\omega_{c'}$ with a probe laser (frequency ω_p) to determine $N_\uparrow$. The strength of the collective measurement is characterized by the average number of probe photons M_t transmitted through the cavity. The probe provides collective population information corresponding to the total number of atoms in $|\uparrow\rangle$, without providing individual atomic state information.

The information gained from a pre-measurement of $\hat{N}_\uparrow$ causes back-action on the system, as illustrated in Fig. 1d. First, the measurement reduces the collective spin projection uncertainty to $\Delta J_z = \Delta N_{\uparrow m}$, where $\Delta N_{\uparrow m}$ is the measurement imprecision. The Heisenberg uncertainty relationship requires fundamental back-action to appear in the orthogonal spin projection $\Delta J_y \geq (N/4)/\Delta N_{\uparrow m}$, referred to as anti-squeezing. Because J_z is not coupled to the back-action quadrature J_y, the ideal measurement is intrinsically back-action evading[35].

However, real systems experience at least two additional sources of probe-induced back-action, which are also illustrated in Fig. 1d.

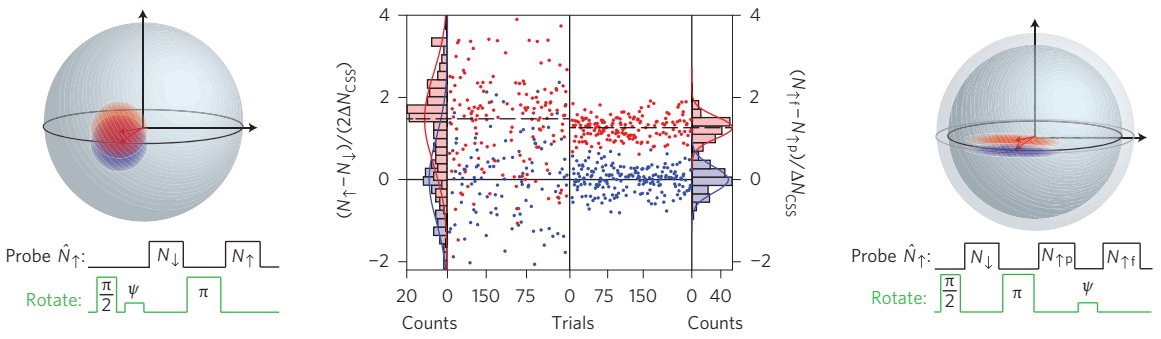

Figure 2 | Detection of a quantum phase with entanglement-enhanced sensitivity. We apply a small rotation ψ to the polar angle θ of both a CSS and a spin-squeezed state, with data and representative Bloch vectors shown on the left and right, respectively. Bloch vectors are not shown to scale. Red data points show experimental trials with $\psi = 2.3(1)$ mrad and blue data points show trials with $\psi = 0$. The data are represented both as histograms and Gaussian curves generated from the average and standard deviation of the measurements. The experimental timing sequence consists of probe pulses (black) and microwave rotations of the Bloch vector polar angle in radians (green). The first measurement of $\hat{N}_\uparrow$ is labelled $N_\downarrow$ as it corresponds to the total population in $|\downarrow\rangle$ after the microwave π-pulse swaps the populations, and gives the total atom number $N = N_\uparrow + N_\downarrow$. For the CSS, the rotation ψ is applied immediately after preparing the CSS along $\hat{x}$. The rotation ψ appears as a change in the quantity $N_\uparrow - N_\downarrow$, which is normalized to the total projection noise that appears in this differential quantity. In the case of the spin-squeezed state, we perform the rotation ψ after a pre-measurement $N_{\uparrow p}$. The rotation then appears as a change in $N_{\uparrow f} - N_{\uparrow p}$, where the projection noise largely cancels. The spin-squeezed state has a spectroscopic enhancement of $W^{-1} = 7.5(9)$, even though the change in $N_{\uparrow f} - N_{\uparrow p}$ is slightly smaller than in the CSS, shown by the dashed black lines. The slight reduction in signal is represented as the smaller Bloch sphere for the spin-squeezed state.

Both are caused by photons spontaneously scattered from the probe into free space, with the average number of scattered photons M_s scaling linearly with the measurement strength $M_s \propto M_t$. One source of back-action arises from free-space scattered photons leaking single-atom information to the environment, projecting an individual atom into $|\uparrow\rangle$ for every free-space scattered photon. For a Bloch vector oriented along $\hat{x}$ as we consider here, this is equivalent to a shortening of the Bloch vector length J such that a subsequent angular deflection θ will produce a reduced change of the measured population $N_{\uparrow f}$.

Another source of probe-induced back-action is spontaneous Raman transitions between ground states driven by the same free-space scattering. Quantum randomness in the number of transitions between states adds noise to the measurement of $\hat{N}_\uparrow$ as the population diffuses amongst ground states. The added noise $\Delta N_{\uparrow D}$ scales as $(\Delta N_{\uparrow D})^2 \propto pM_t$, where p is the probability for an atom to undergo a ground-state changing transition when it scatters a photon into free space. The optimum spin-noise reduction R is fundamentally limited by the need to balance the decrease in measurement noise $\Delta N_{\uparrow m} \propto 1/\sqrt{M_t}$ versus the increase in diffusion noise $\Delta N_{\uparrow D} \propto \sqrt{M_t}$. This balancing is analogous to radiation pressure back-action, which sets the SQL for measurements of mechanical position[35].

The key experimental advance in this work is the elimination of state-changing transitions as a limitation on W. This is achieved by creating a system in which collective coupling to the probe mode is enhanced relative to single-atom processes. Our approach uses a medium finesse $F = 660$ optical cavity to enhance the collective coupling, with the figure of merit $NC \approx 6 \times 10^3$, where $C = 1.1(1) \times 10^{-2}$ is the single-atom cooperativity[19,21]. In addition, we suppress state-changing transitions by using σ^+ polarized probe light on a cycling transition[18,34,36,37]. Thus, the probability p is reduced by a factor of 150 from that of our previous work[21]. As a result, previously ignored noise sources, not yet fully understood (see Supplementary Section VI), now dominate the probe-induced back-action on measurement $\hat{N}_\uparrow$.

Direct observation of spectroscopic enhancement

In Fig. 2 we directly sense an externally applied phase shift with a resolution significantly below the SQL. We apply a small rotation ψ of the polar angle θ using a microwave pulse, as described in Supplementary Section III. In one case, the rotation is applied to a CSS with no pre-measurement. In the second case, the rotation is applied just after the pre-measurement of $\hat{N}_\uparrow$, which prepares a conditional spin-squeezed state. The deflection of $N_{\uparrow f}$ is slightly smaller for the spin-squeezed state due to probe-induced collapse during the pre-measurement $N_{\uparrow p}$. However, the reduction in noise in the quantity $N_{\uparrow f} - N_{\uparrow p}$ allows the rotation angle to be estimated with an enhancement $W^{-1} = 7.5(9)$ in this example data set, with measurement strength $M_t = 2.7(1) \times 10^4$ and $N = 4.3 \times 10^5$. No background subtractions or corrections are applied. In a single shot, the fractional error rate in determining whether the phase shift of $\psi = 2.3(1)$ mrad was applied is reduced from 0.27(1) without the pre-measurement to 0.022(7) with the pre-measurement.

The probe light during the pre-measurement produces large inhomogeneous light shifts that strongly dephase the Bloch vector, resulting in a loss of sensitivity for detecting any applied rotations after the pre-measurement $N_{\uparrow p}$. We remove the dephasing caused by the measurement by inserting an extra, unused measurement labelled $N_\downarrow$ and a π-pulse before the pre-measurement, essentially spin-echoing away the dephasing and restoring the sensitivity to applied rotations.

More generally, we can identify an optimum spectroscopic enhancement by measuring both the spin noise reduction R and the fractional shortening of the Bloch vector $\mathcal{C} = J/(N/2)$ as a function of measurement strength M_t (shown in Fig. 3a). First, we consider the spin noise reduction. The maximum R^{-1} observed, with no background subtraction, is $R^{-1} = 16(2)$ at $M_t = 4.1 \times 10^4$. The contributions of various noise sources are quantified using a fit to the observed R versus M_t. The model $R = r_{PSN}/M_t + R_{tf} + r_q M_t + r_c M_t^2$, includes four noise contributions: photon shot noise r_{PSN}, a technical noise floor $R_{tf}^{-1} = 73(34)$ independent of M_t, probe-induced quantum back-action r_q and probe-induced classical back-action r_c. Photon shot noise dominates at low M_t, so that R^{-1} initially increases as M_t increases. However, the rise in classical back-action $r_c M_t^2$ eventually limits R^{-1}. At the optimum M_t, the classical back-action r_c alone would limit R^{-1} to 67(15). The quantum back-action r_q is statistically consistent with zero.

We have effectively eliminated ground-state transitions as a substantial source of back-action in the current experiment. The noise added due to population diffusion from state-changing transitions is estimated to only limit R^{-1} to $1.7(3) \times 10^3$ as measured by

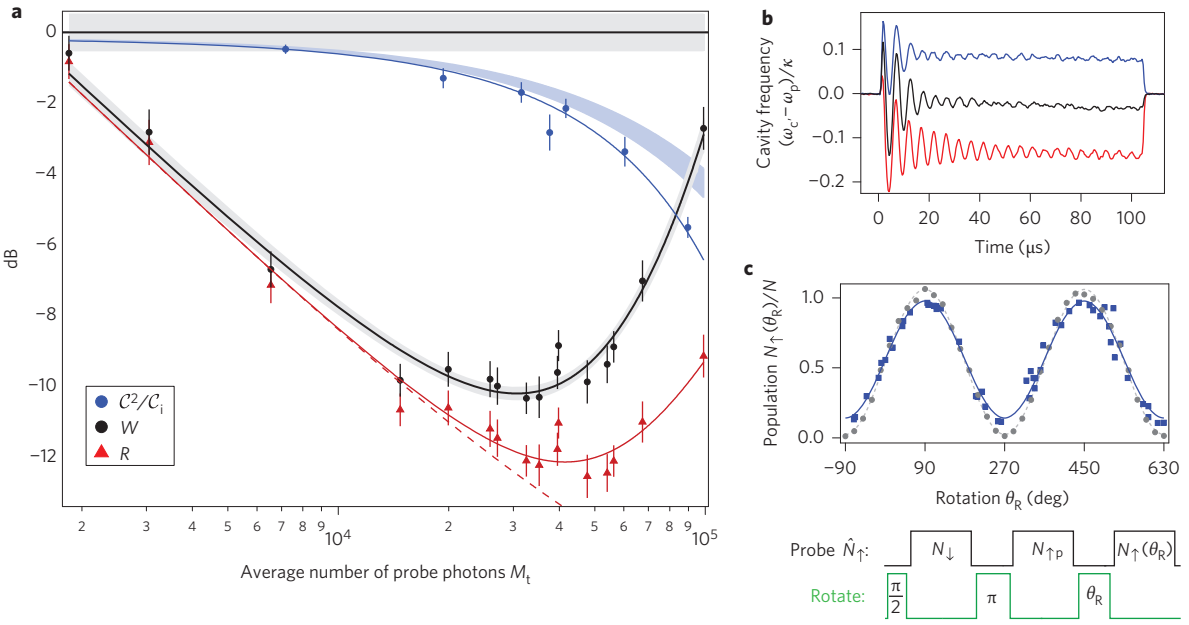

Figure 3 | Spin-squeezing and probe-induced back-action. a, Scaling of the spin noise reduction R (red), loss of signal $\mathcal{C}^2/\mathcal{C}_i$ (blue) and the inverse of the spectroscopic enhancement W (black) versus probe intensity M_t for $N = 4.8 \times 10^5$. The red, blue and black curves are fits to the data. The data for W are calculated from R data and the fit to $\mathcal{C}^2/\mathcal{C}_i$. The 68% confidence band for the W fit and the SQL is in grey. The dashed red curve shows the fitted R assuming no probe-induced added noise ($r_c = r_q = 0$). The light-blue region is the predicted $\mathcal{C}^2/\mathcal{C}_i$ due to free-space scattering. All error bars represent 1 s.d. We use the usual convention for expressing a ratio X in dB units, $x(\text{dB}) = 10\log_{10}X$. **b**, Examples of optomechanical oscillations in the dressed cavity frequency $\omega_{c'}$. The relative detuning of $\omega_{c'}$ and ω_p results in increased ($\omega_{c'} > \omega_p$, blue) or decreased ($\omega_{c'} < \omega_p$, red) oscillation damping rates, a source of probe-induced back-action noise (see Supplementary Section VI). Each curve is the average of 30 experimental trials. **c**, Example data and experimental sequence for the measurement of contrast $\mathcal{C}$. Probe pulses (black) are measurements of $\hat{N}_\uparrow$. The first measurement is labelled $N_\downarrow$ as it corresponds to the total population in $|\downarrow\rangle$ after the microwave π-pulse swaps the populations. Microwave pulses (green) rotate the polar angle θ of the Bloch vector. After a pre-measurement labelled $N_{\uparrow p}$, a variable rotation θ_R is applied and $N_\uparrow(\theta_R)$ is recorded. Contrast $\mathcal{C}$ is determined from the amplitude of the $N_\uparrow(\theta_R)$ fringe (curves are a fit to the data), with two examples shown in blue and grey for $M_t = 3.0 \times 10^4$ and $M_t = 0$, respectively.

probe-induced optical pumping between different ground states (see Supplementary Section V). Also, the inferred contribution to r_c due to the observed classical fluctuations in probe power would only limit R^{-1} to $3.2(4) \times 10^4$. The equivalent transition probability is $p \leq 4.4(8) \times 10^{-3}$. For comparison, the clock states in our previous work had a transition probability $p = 2/3$, which, in our current system, would limit R^{-1} to 1.9(2). With population noise considerably suppressed, other sources of back-action, including optomechanical effects (Fig. 3b), appear to dominate the probe-induced back-action on R.

Free-space scattering also leads to a reduction in the Bloch vector length J and the resulting loss of signal must be accounted for to determine the spectroscopic enhancement. To determine J, the polar angle of the Bloch vector θ is varied after the pre-measurement $N_{\uparrow p}$ using a microwave pulse. The population $N_\uparrow$ is then recorded versus the rotation angle (Fig. 3c). The fractional reduction in length of the Bloch vector is determined from the fitted contrast $\mathcal{C} = 2J/N$ of the observed fringe. The initial contrast at $M_t = 0$ is $\mathcal{C}_i = 0.97(3)$ and $\mathcal{C}$ monotonically decreases as a function of M_t, close to the limit from wavefunction collapse due to free-space scattering (Fig. 3a). We believe uncancelled inhomogeneous probe light shifts are responsible for the additional small loss of contrast (see Supplementary Section IV).

Taken together, the decrease in spin noise and loss of contrast quantify the spectroscopic enhancement of the spin-squeezed state $W^{-1} = R^{-1}\mathcal{C}^2/\mathcal{C}_i$, as calculated in refs 18, 19 and 21. The optimum observed improvement corresponds to $W^{-1} = 10.5(1.5)$ or 10.2(6) dB. This value includes no measurement background noise subtraction, and thus represents the actual realized improvement in phase sensitivity.

Further confirmation that our collective measurement is near the cycling transition limit is the observed $\Delta\theta^2 \propto 1/N^2$ scaling of the absolute phase resolution[18,34] (Fig. 4). For comparison, the optimal phase resolution when state-changing processes are the dominant limitation on W scales as $N^{-3/2}$. This more favourable scaling with N is important in practical applications for which the absolute phase resolution is the key figure of merit.

Discussion

When the spectroscopic enhancement W^{-1} is ≥1, the ensemble is guaranteed to be entangled. Maximally entangled ensembles can achieve a phase estimation precision of $\Delta\theta^2_{HL} = 1/N^2$, known as the Heisenberg limit, which has been realized with small ensembles[25]. Although our system is far from the Heisenberg limit for $N = 4.8 \times 10^5$ atoms, the absolute phase sensitivity is equivalent to ~44,000 copies of an entangled 11-atom ensemble at the Heisenberg limit. Such a comparison emphasizes the massive parallelism achievable by collective measurements to generate entanglement in neutral atom ensembles.

The optical nature of our approach, among other experimentally demonstrated[18–20,22,33] and theoretically proposed[38] approaches, offers the advantage that the probe or squeezing laser can be completely extinguished after the squeezed state is generated. In contrast, a potential challenge for squeezing generated using atomic collisions is whether the interactions that generate entanglement can be sufficiently reduced to avoid loss of accuracy and precision during the subsequent sensing period. For this reason, our approach may be compatible with a wide array of atomic sensors, and may be particularly well suited for optical lattice clocks[11,12], which have already begun to incorporate optical cavities[39]. Although state-of-the-art

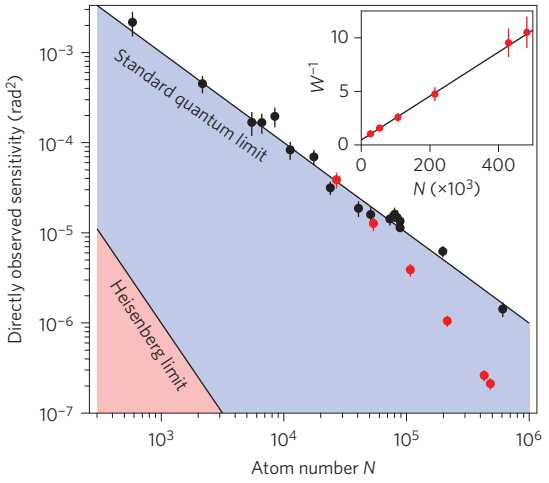

Figure 4 | Absolute phase sensitivity versus *N*. Red points are the observed variance in phase estimation for spin-squeezed states, optimized with respect to measurement strength M_t, for different atom numbers N. The data show the predicted $1/N^2$ scaling for probing on a cycling transition[34,36], equivalent to a linear scaling of the spectroscopic enhancement W^{-1} versus N, shown in the inset. The black line is a linear fit to the data. The SQL is confirmed by measuring the projection noise that appears in $N_\downarrow - N_{\uparrow p}$ (black points, each 100 trials) and observing $1/N$ scaling in of the variance. Error bars indicate 68.3% confidence intervals.

optical lattice clocks[11,12] use smaller atom numbers and densities than are used in this work in order to avoid density-dependent systematic errors, it should be possible to achieve the same amount of enhancement demonstrated here. Approaches may include utilizing higher-finesse cavities, achieving a higher probe detection efficiency, or utilizing a three-dimensional lattice trap[40] to scale up to larger atom numbers, which has the added benefit that the standard quantum limit on phase resolution would also be reduced. Finally, the low-noise, non-destructive readout method is useful for purely classical, but substantial, improvements in the measurement duty cycle of lattice clocks and other atomic sensors[41].

Straightforward technical improvements could both decrease the technical measurement noise floor and increase the total probe detection efficiency from 8(5)% to >50%, allowing us to reach $W^{-1} \approx 100$ in our current system with only a medium-finesse optical cavity. In addition to demonstrating a large spectroscopic enhancement relevant for state-of-the-art atomic sensors, the results here also uncover previously unimportant forms of probe-induced back-action, such as heating of the atomic motion. Further study of these forms of probe-induced back-action will likely be required to realize even further spectroscopic enhancement.

Note added in proof: After completion of this manuscript, a paper inferring comparable spectroscopic enhancement via atomic collisions was reported[42]. A modest background subtraction was applied to infer the reported value.

Received 12 February 2014; accepted 11 June 2014; published online 13 July 2014

References

1. Olmschenk, S. *et al.* Quantum teleportation between distant matter qubits. *Science* **323,** 486–489 (2009).
2. Kok, P. *et al.* Linear optical quantum computing with photonic qubits. *Rev. Mod. Phys.* **79,** 135–174 (2007).
3. Eckert, K. *et al.* Quantum non-demolition detection of strongly correlated systems. *Nature Phys.* **4,** 50–54 (2007).
4. Dicke, R. H. Coherence in spontaneous radiation processes. *Phys. Rev.* **93,** 99–110 (1954).
5. Guerlin, C. *et al.* Progressive field-state collapse and quantum non-demolition photon counting. *Nature* **448,** 889–893 (2007).
6. Ristè, D. *et al.* Deterministic entanglement of superconducting qubits by parity measurement and feedback. *Nature* **502,** 350–354 (2013).
7. Chou, C. W. *et al.* Measurement-induced entanglement for excitation stored in remote atomic ensembles. *Nature* **438,** 828–832 (2005).
8. Kuzmich, A., Bigelow, N. P. & Mandel, L. Atomic quantum non-demolition measurements and squeezing. *Europhys. Lett.* **42,** 481–486 (1998).
9. Kominis, I. K., Kornack, T. W., Allred, J. C. & Romalis, M. V. A subfemtotesla multichannel atomic magnetometer. *Nature* **422,** 596–599 (2003).
10. Gustavson, T. L., Bouyer, P. & Kasevich, M. A. Precision rotation measurements with an atom interferometer gyroscope. *Phys. Rev. Lett.* **78,** 2046–2049 (1997).
11. Hinkley, N. *et al.* An atomic clock with 10^{-18} instability. *Science* **341,** 1215–1218 (2013).
12. Bloom, B. J. *et al.* An optical lattice clock with accuracy and stability at the 10^{-18} level. *Nature* **506,** 71–75 (2014).
13. Orzel, C. Searching for new physics through atomic, molecular and optical precision measurements. *Phys. Scripta* **86,** 068101–68109 (2012).
14. Itano, W. *et al.* Quantum projection noise: population fluctuations in two-level systems. *Phys. Rev. A* **47,** 3554–3570 (1993).
15. Eichler, C. *et al.* Observation of two-mode squeezing in the microwave frequency domain. *Phys. Rev. Lett.* **107,** 113601 (2011).
16. Eberle, T. *et al.* Quantum enhancement of the zero-area Sagnac interferometer topology for gravitational wave detection. *Phys. Rev. Lett.* **104,** 251102 (2010).
17. Wineland, D. J., Bollinger, J. J., Itano, W. M., Moore, F. L. & Heinzen, D. J. Spin squeezing and reduced quantum noise in spectroscopy. *Phys. Rev. A* **46,** R6797–R6800 (1992).
18. Appel, J. *et al.* Mesoscopic atomic entanglement for precision measurements beyond the standard quantum limit. *Proc. Natl Acad. Sci. USA* **106,** 10960–10965 (2009).
19. Schleier-Smith, M. H., Leroux, I. D. & Vuletić, V. States of an ensemble of two-level atoms with reduced quantum uncertainty. *Phys. Rev. Lett.* **104,** 073604 (2010).
20. Wasilewski, W. *et al.* Quantum noise limited and entanglement-assisted magnetometry. *Phys. Rev. Lett.* **104,** 133601 (2010).
21. Chen, Z., Bohnet, J. G., Sankar, S. R., Dai, J. & Thompson, J. K. Conditional spin squeezing of a large ensemble via the vacuum Rabi splitting. *Phys. Rev. Lett.* **106,** 133601 (2011).
22. Sewell, R. J. *et al.* Magnetic sensitivity beyond the projection noise limit by spin squeezing. *Phys. Rev. Lett.* **109,** 253605 (2012).
23. Meyer, V. *et al.* Experimental demonstration of entanglement-enhanced rotation angle estimation using trapped ions. *Phys. Rev. Lett.* **86,** 5870–5873 (2001).
24. Leibfried, D. *et al.* Creation of a six-atom 'Schrödinger cat' state. *Nature* **438,** 639–642 (2005).
25. Monz, T. *et al.* 14-Qubit entanglement: creation and coherence. *Phys. Rev. Lett.* **106,** 130506 (2011).
26. Noguchi, A., Toyoda, K. & Urabe, S. Generation of Dicke states with phonon-mediated multilevel stimulated Raman adiabatic passage. *Phys. Rev. Lett.* **109,** 260502 (2012).
27. Estève, J., Gross, C., Weller, A., Giovanazzi, S. & Oberthaler, M. K. Squeezing and entanglement in a Bose–Einstein condensate. *Nature* **455,** 1216–1219 (2008).
28. Riedel, M. F. *et al.* Atom-chip-based generation of entanglement for quantum metrology. *Nature* **464,** 1170–1173 (2010).
29. Gross, C., Zibold, T., Nicklas, E., Estève, J. & Oberthaler, M. K. Nonlinear atom interferometer surpasses classical precision limit. *Nature* **464,** 1165–1169 (2010).
30. Bücker, R. *et al.* Twin-atom beams. *Nature Phys.* **7,** 608–611 (2011).
31. Lücke, B. *et al.* Twin matter waves for interferometry beyond the classical limit. *Science* **334,** 773–776 (2011).
32. Hamley, C. D., Gerving, C. S., Hoang, T. M., Bookjans, E. M. & Chapman, M. S. Spin nematic squeezed vacuum in a quantum gas. *Nature Phys.* **8,** 305–308 (2012).
33. Leroux, I. D., Schleier-Smith, M. H. & Vuletić, V. Implementation of cavity squeezing of a collective atomic spin. *Phys. Rev. Lett.* **104,** 073602 (2010).
34. Chen, Z., Bohnet, J. G., Weiner, J. M., Cox, K. C. & Thompson, J. K. Cavity-aided nondemolition measurements for atom counting and spin squeezing. *Phys. Rev. A* **89,** 043837 (2014).
35. Braginsky, V. B., Vorontsov, Y. I. & Thorne, K. S. Quantum nondemolition measurements. *Science* **209,** 547–557 (1980).
36. Saffman, M., Oblak, D., Appel, J. & Polzik, E. S. Spin squeezing of atomic ensembles by multicolor quantum nondemolition measurements. *Phys. Rev. A* **79,** 023831 (2009).
37. Zhang, H. *et al.* Collective state measurement of mesoscopic ensembles with single-atom resolution. *Phys. Rev. Lett.* **109,** 133603 (2012).
38. Gil, L. I. R., Mukherjee, R., Bridge, E. M., Jones, M. P. A. & Pohl, T. Spin squeezing in a Rydberg lattice clock. *Phys. Rev. Lett.* **112,** 103601 (2014).
39. Nicholson, T. L. *et al.* Comparison of two independent Sr optical clocks with 1×10^{-17} stability at 10^3 s. *Phys. Rev. Lett.* **109,** 230801 (2012).

40. Westergaard, P. G. *et al.* Lattice-induced frequency shifts in Sr optical lattice clocks at the 10^{-17} level. *Phys. Rev. Lett.* **106,** 210801 (2011).
41. Westergaard, P., Lodewyck, J. & Lemonde, P. Minimizing the Dick effect in an optical lattice clock. *IEEE Trans. Ultrason. Ferroelectr. Freq. Control* **57,** 623–628 (2010).
42. Lücke, B. *et al.* Detecting multiparticle entanglement of Dicke states. *Phys. Rev. Lett.* **112,** 155304 (2014).

Acknowledgements

The authors acknowledge K. McAlpine's early contributions to building detectors and helpful discussions with A. M. Rey and K. W. Lehnert. The authors acknowledge financial support from the Defense Advanced Research Projects Agency Quantum Assisted Sensing and Readout project (DARPA QuASAR), the Army Research Office (ARO), the National Science Foundation Physics Frontier Center (NSF PFC) and the National Institute of Standards and Technology (NIST). J.G.B. acknowledges support from the National Science Foundation Graduate Research Fellowship (NSF GRF) and K.C.C. acknowledges support from the National Defense Science and Engineering Fellowship (NDSEG). This material is based upon work supported by the National Science Foundation (grant no. 1125844).

Author contributions

J.G.B., K.C.C., M.A.N. and J.M.W. designed and performed experiments and analysed data. Z.C. provided analytic support. J.K.T. designed the experiment and analysed data. J.G.B. wrote the manuscript and all authors provided feedback for the manuscript.

Additional information

Supplementary information is available in the online version of the paper. Reprints and permissions information is available online at www.nature.com/reprints. Correspondence and requests for materials should be addressed to J.K.T.

Competing financial interests

The authors declare no competing financial interests.